

# Expanding Carbon Capture Capacity: Uncovering Additional CO<sub>2</sub> Adsorption Sites in Imine-Linked Porous Organic Cages Supporting Information

Zezhong John Li, Simcha Srebnik\*

\*Email: simcha.srebnik@ubc.ca

Department of Chemical & Biological Engineering, University of British Columbia, 2360 East  
Mall, Vancouver, B.C., Canada V6T 1Z3

## Table of Contents

Force field equations.....	2
Force field parameters.....	3
Sensitivity analysis on the number of CO <sub>2</sub> in the simulation box .....	7
Additional CO <sub>2</sub> density and potential energy mapping .....	8
MD simulation visualization.....	9
Mapping methodology .....	10
Nomenclatures .....	12
References.....	13
SI Video file: An externally adsorbed CO <sub>2</sub> replacing an internally adsorbed CO <sub>2</sub>	

## Force field equations

### 1. Intermolecular interactions

- Lennard-Jones:  $v_{LJ}(r) = 4\varepsilon\left[\left(\frac{\sigma}{r}\right)^{12} - \left(\frac{\sigma}{r}\right)^6\right]$
- Coulomb:  $v_{zz}(r_{ij}) = \frac{z_i z_j}{4\pi\varepsilon_0 r_{ij}}$

### 2. Intramolecular interactions

- Bond:  $v_b(r) = k_b(r - r_0)^2$
- Angle:  $v_a(\theta) = k_a(\theta - \theta_0)^2$
- Dihedral:  $v_d(\theta) = 0.5k_1(1 + \cos(\theta)) + 0.5k_2(1 - \cos(2\theta)) + 0.5k_3(1 + \cos(3\theta)) + 0.5k_4(1 - \cos(4\theta))$
- Improper:  $v_{im}(\theta) = 0.5k_{im}(1 - \cos(2\theta))$

## Force field parameters

The specific OPLS-UA force field parameters for the crown-ether-substituted cage were mainly selected from the Tinker Molecular Modelling database (V8.7) with the individual charge scaled to provide an electrically neutral cage molecule. The choice of atom types and force field parameters was further adjusted according to literature values.<sup>1</sup> The force field parameters of CO<sub>2</sub> were adopted from Cygan *et al.*,<sup>2</sup> who conducted parametric optimization through a series of molecular dynamics simulations and power spectrum calculations. These were based on the original expanded potentials of Zhu *et al.*,<sup>3</sup> stemming from the earlier work of Harris and Yung.<sup>4</sup> The force field parameters of CO<sub>2</sub> were previously successfully used in MD simulation of CO<sub>2</sub> adsorption in porous materials.<sup>2</sup> The labeling of each type of atom of the POC is shown in **Figure S1**.

### 1. CO<sub>2</sub> parameter

Table S1. Atom type parameters for CO<sub>2</sub>

Atom Type	Mass	Charge [e]	$\sigma$ [Å]	$\epsilon$ [kcal mol <sup>-1</sup> ]
C	12.01070	0.6512	2.800	0.05593
O	15.99900	-0.3256	3.028	0.15973

Table S2. Bond stretching parameters for CO<sub>2</sub>

Bond Type	$k_b$ [kcal mol <sup>-1</sup> Å <sup>-2</sup> ]	$l_0$ [Å]
C-O	1008.9625	1.162

Table S3. Angle bending parameters for CO<sub>2</sub>

Angle Type	$k_a$ [kcal mol <sup>-1</sup> rad <sup>-2</sup> ]	$\theta_0$ [degree]
O-C-O	54.0033	180

## 2. Crown-ether-substituted cage parameters

Table S4. Atom type parameters for cage molecule

Atom Type	Mass	Charge [e]	$\sigma$ [Å]	$\epsilon$ [kcal mol <sup>-1</sup> ]
CH	13.0190	0.2200	0.0800	3.8500
C8	13.0190	0.1150	0.1150	3.8000
CD	13.0190	0.0000	0.1100	3.7500
OS	15.9990	-0.5000	0.1700	3.0000
C2	14.0270	0.2500	0.1180	3.8000
CA	12.0110	-0.1150	0.0700	3.5500
NO	14.0070	-0.2200	0.1700	3.2500

Table S5. Bond stretching parameters for cage molecule

Bond Type	$k_b$ [kcal mol <sup>-1</sup> Å <sup>-2</sup> ]	$l_0$ [Å]
C2-C2	260	1.526
CH-C2	260	1.526
C2-OS	320	1.425
CH-CH	260	1.526
NO-CH	337	1.449
C8-NO	529	1.250
CA-CD	469	1.400
CA-C8	427	1.433

Table S6. Angle bending parameters for cage molecule

Angle Type	$k_a$ [kcal mol <sup>-1</sup> rad <sup>-1</sup> ]	$\theta_0$ [degree]
OS-C2-C2	80	109.5
CH-C2-OS	80	109.5
CH-CH-C2	63	111.5
NO-CH-C2	80	109.7
NO-CH-CH	80	109.7
CA-C8-NO	70	120.0
C2-OS-C2	100	111.8
C8-NO-CH	50	118.0
CD-CA-CD	85	120.0
CD-CA-C8	70	120.0
CA-CD-CA	63	120.0

Table S7. Dihedral parameters for cage molecule

Dihedral Type	$k_1$ [kcal mol <sup>-1</sup> ]	$k_2$ [kcal mol <sup>-1</sup> ]	$k_3$ [kcal mol <sup>-1</sup> ]	$k_4$ [kcal mol <sup>-1</sup> ]
NO-CH-CH-NO	1.428	0.086	0.029	0
CD-CA-C8-NO	1.241	3.353	-0.286	0
C2-CH-CH-C2	1.300	-0.050	0.200	0
CH-CH-C2-OS	1.300	-0.050	0.200	0
NO-CH-CH-C2	0.845	-0.962	0.713	0
OS-C2-C2-OS	-0.550	0	0	0
CH-C2-OS-C2	0.650	-0.250	0.670	0
C8-NO-CH-CH	4.753	-0.734	0	0
C8-CA-CD-CA	0	7.250	0	0
CD-CA-CD-CA	0	7.250	0	0
CA-C8-NO-CH	0	23.900	0	0

Table S8. Improper parameter for cage molecule

Improper Type	$k_{im}$ [kcal mol <sup>-1</sup> ]
C8-CA-CD-CD	5

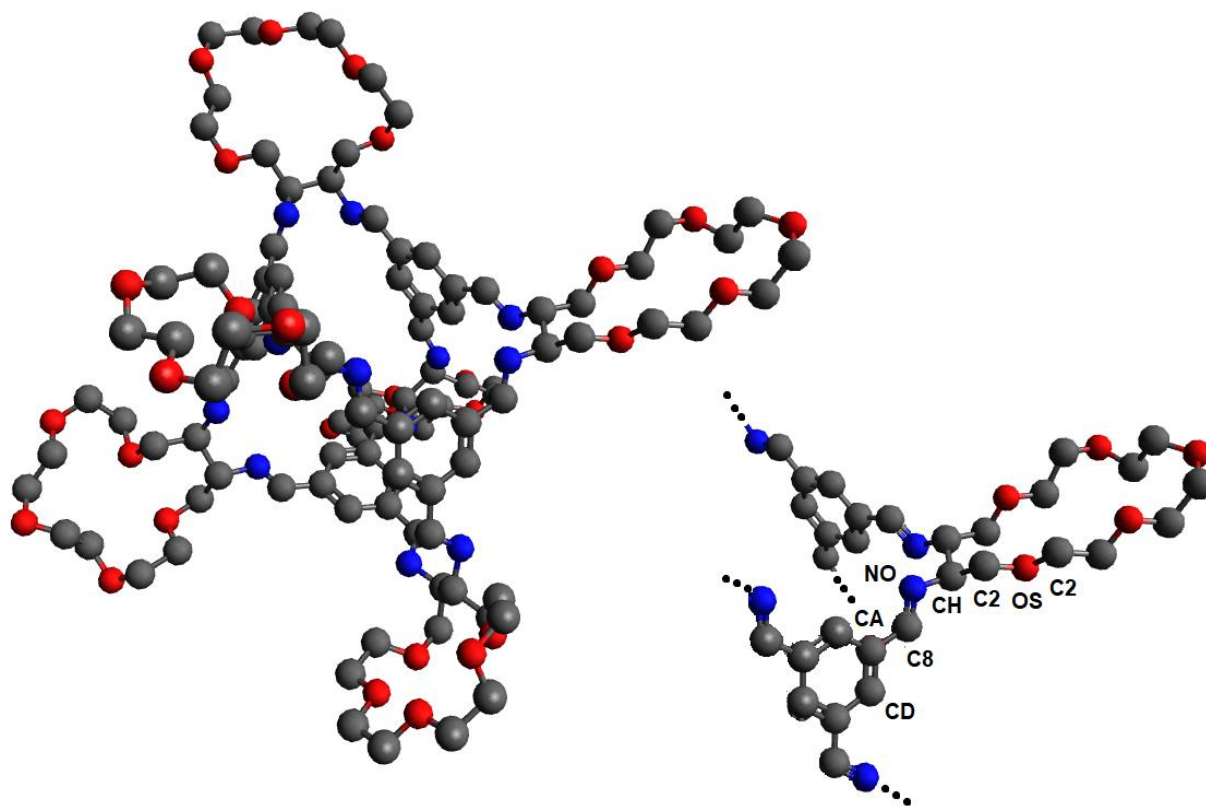


Figure S1. Schematics of the crown-ether-substituted cage structure with the repeating unit label with the atom types used in force field definition.

## Sensitivity analysis on the number of CO<sub>2</sub> in the simulation box

**Figure S2** compares the cumulative CO<sub>2</sub> uptake as a function of radial distance from the centre of cage cavity at four different number of CO<sub>2</sub> molecules in the simulation box. It is shown that the gas uptake become independent of the number of CO<sub>2</sub> with greater or equal to 20 CO<sub>2</sub> molecules. Hence, 20 CO<sub>2</sub> was selected for this simulation for efficiency.

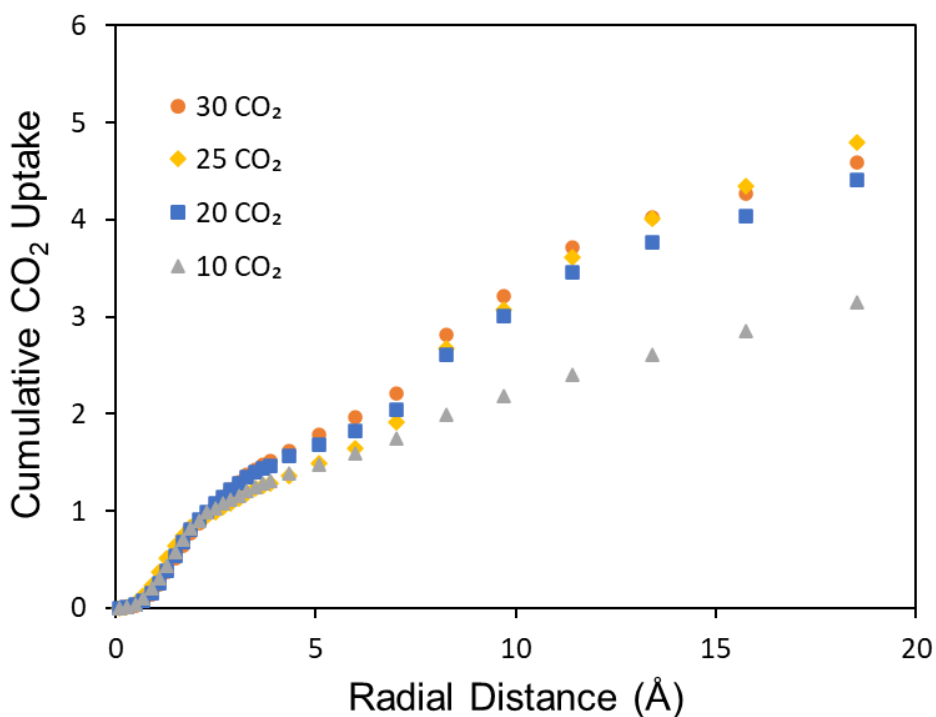


Figure S2. The cumulative CO<sub>2</sub> uptake as a function of radial distance from the centre of cage cavity at four different number of CO<sub>2</sub> molecules in the simulation box

## Additional CO<sub>2</sub> density and potential energy mapping

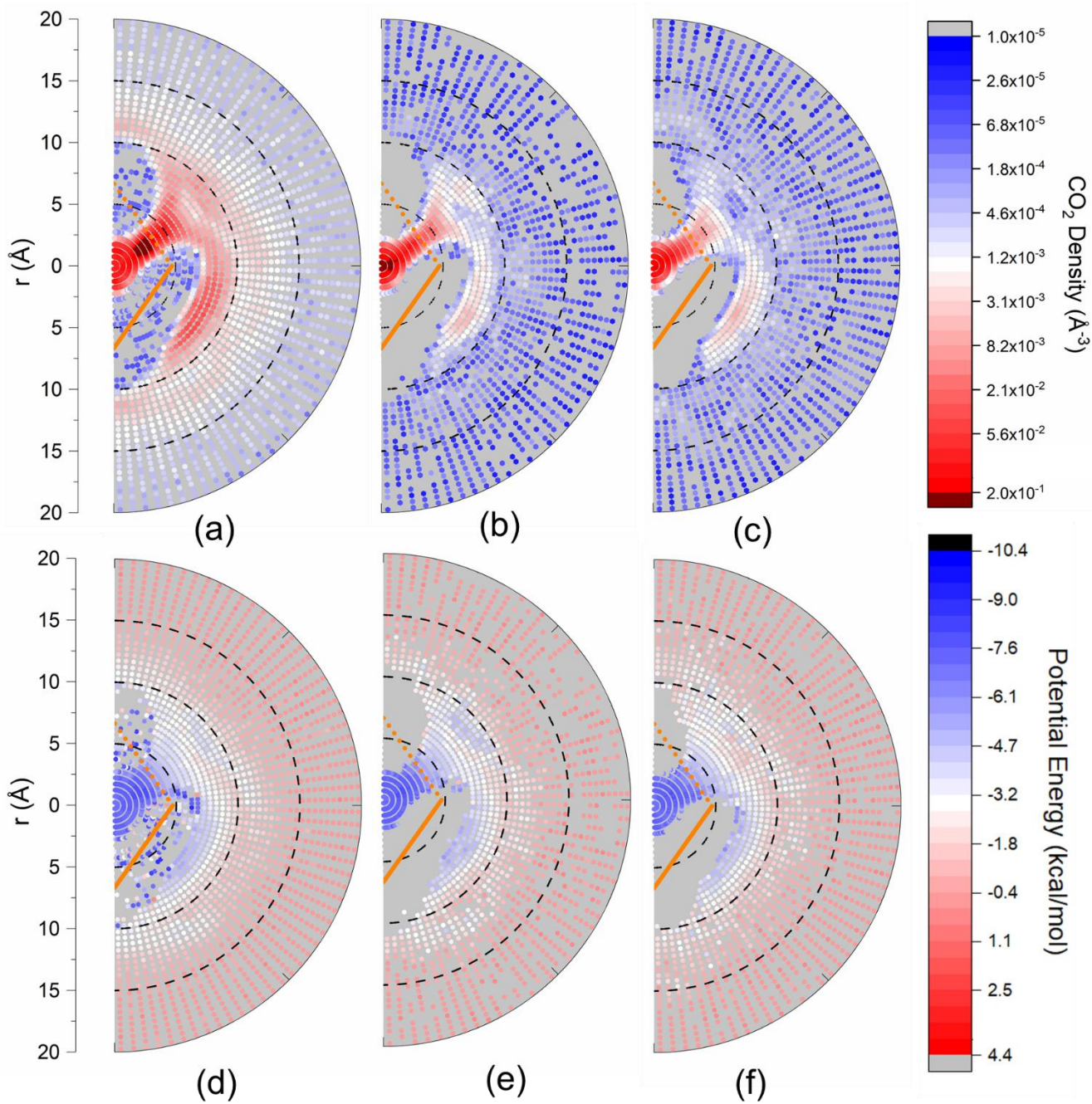


Figure S3. The local CO<sub>2</sub> density mapping at (a) 300 K 4 atm, (b) 300 K 0.5 atm and (c) 350 K 1 atm, and the intermolecular potential energy mapping between CO<sub>2</sub> molecules and the cage molecule at (d) 300 K 4 atm, (e) 300 K 0.5 atm and (f) 350 K 1 atm.

## MD simulation visualization

The simulation results were visualized using Visual Molecular Dynamics (VMD) software (V1.9).<sup>5</sup> The position and the motion of molecules was visually examined, providing directions for quantitative data processing. **Figure S4** shows an example of the visualization of the simulation results at 350 K and 1 atm, where 2 CO<sub>2</sub> molecules are seen inside the cage cavity and many more are found surrounding the cage molecule. A video clip of the visualization of the simulation at 250 K and 1 atm is included in the **Supporting Information video file** to show how an externally adsorbed CO<sub>2</sub> molecule replaces an internally adsorbed CO<sub>2</sub> molecule.

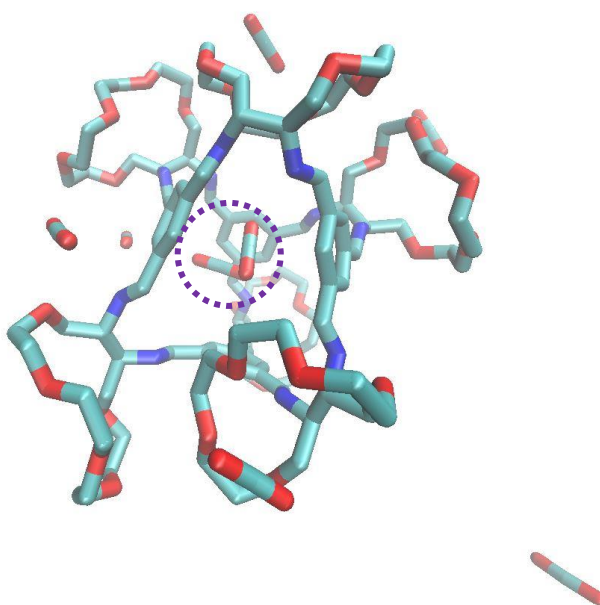


Figure S4. A representative visualization of the simulation results at 250 K and 1 atm where oxygen is in red, nitrogen is in blue and carbon is in cyan. Hydrogen atoms in the ether-substituted POC are omitted due to the choice of OPLS-UA force field. The two CO<sub>2</sub> molecules inside the cage cavity are highlighted in the purple dashed circle.

## Mapping methodology

The CO<sub>2</sub> density and potential energy were mapped in this set of newly defined Cartesian coordinates whose origin is the centre of mass of the cage base and the three coordinates go through the three vertices of the cage base. **Figure S5** illustrates how such coordinates were defined. Here, the blue dashed lines outline the cage base (i.e. the part excluding 6 vertex functional groups in **Figure S5a**), the yellow dashed lines with arrows represent the axes of the new Cartesian coordinates and the green dot represents the centre of mass of the cage base. The location of each CO<sub>2</sub> molecule was calculated with respect to this new coordinate system by vector transformation using linear algebra. After coordinate conversion, the mapping region (pink semicircles in **Figure 3a** with a thickness of 0.8 Å) was discretized into small intervals in cylindrical coordinates with 60 parts in the angular direction and 40 parts in the radial direction as shown by the dots in **Figure 3b-c**. To be specific, the cylindrical coordinates have an axial direction perpendicular to the pink semicircular regions in **Figure 3a** and is centred at the same origin as the Cartesian coordinates in **Figure 5b**. The appearance of CO<sub>2</sub> molecules was tallied into each interval together with the potential energy between that given CO<sub>2</sub> molecule and the cage molecule. The results in all four semi-circular mapping regions were compiled and averaged after realigning the wall and window locations. The averaged CO<sub>2</sub> density and potential energy data is presented in a semi-circular region like the ones shown in **Figure 3b-c**.

In order to analyze the external adsorption sites, spherical mapping regions were used to reveal the CO<sub>2</sub> density and potential energy at site **2** and **3**. Each wall (**Figure S5c**) or window (**Figure S5d**) corresponds to one eighth of a sphere whose centre coincides with the cage centre. Hence, there are 4 subregions for the 4 cage windows and 4 subregions for the 4 walls. Sphere radius of 8 Å with a thickness of 0.8 Å was selected for the four type **2** sites. Sphere radius of 9 Å

with a thickness of  $0.8 \text{ \AA}$  was selected for the four type **3** sites.  $\text{CO}_2$  appearance at the two types of adsorption sites were tallied into small intervals in the four subregions of eighth sphere corresponding to walls and windows, respectively, together with the potential energy between that given  $\text{CO}_2$  molecule and the cage molecule. Data in all four mapping subregions were reoriented to align the vertices and averaged to obtain the final results presented in this work.

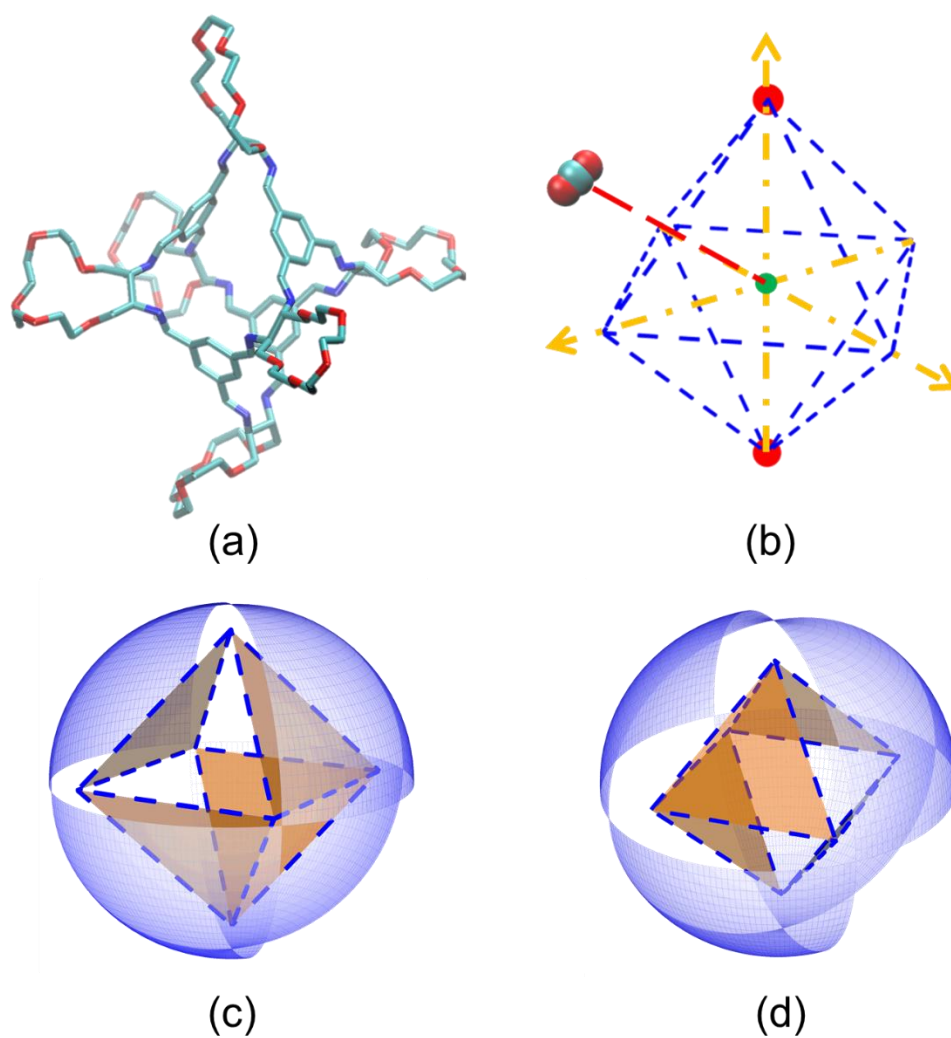


Figure S5. (a) The structure of the 15-crown-5 ether cage and (b) the graphic representation of the new Cartesian coordinates defined based on the geometry of the cage.  $\text{CO}_2$  location is calculated in this new coordinate system. The spherical mapping regions shaded in blue for (c) type **2** wall sites and (d) type **3** window sites.

## Nomenclatures

### Latin alphabet

k	interaction parameter in force field equations
r	interatomic distance
$v$	potential energy due to an individual interatomic interaction
z	partial charge on an atom

### Greek alphabet

$\varepsilon$	depth of the potential well of the Lennard-Jones potential
$\varepsilon_0$	the permittivity of vacuum, $8.854 \times 10^{-12} \text{ F}\cdot\text{m}^{-1}$
$\theta$	angle between two bonds
$\sigma$	equilibrium interatomic distance where the Lennard-Jones potential equals zero

### Subscripts

a	angle interaction
b	bond interaction
d	dihedral interaction
i	generic atom $i$
im	improper interaction
LJ	Lennard-Jones interaction
zz	Coulomb interaction

## References

- (1) Giri, N.; Del Pópolo, M. G.; Melaugh, G.; Greenaway, R. L.; Rätzke, K.; Koschine, T.; Pison, L.; Gomes, M. F. C.; Cooper, A. I.; James, S. L. Liquids with Permanent Porosity. *Nature* **2015**, *527* (7577), 216–220. <https://doi.org/10.1038/nature16072>.
- (2) Cygan, R. T.; Romanov, V. N.; Myshakin, E. M. Molecular Simulation of Carbon Dioxide Capture by Montmorillonite Using an Accurate and Flexible Force Field. *J. Phys. Chem. C* **2012**, *116* (24), 13079–13091. <https://doi.org/10.1021/jp3007574>.
- (3) Zhu, A.; Zhang, X.; Liu, Q.; Zhang, Q. A Fully Flexible Potential Model for Carbon Dioxide. *Chinese J. Chem. Eng.* **2009**, *17* (2), 268–272. [https://doi.org/10.1016/S1004-9541\(08\)60204-9](https://doi.org/10.1016/S1004-9541(08)60204-9).
- (4) Harris, J. G.; Yung, K. H. Carbon Dioxide's Liquid-Vapor Coexistence Curve and Critical Properties as Predicted by a Simple Molecular Model. *J. Phys. Chem.* **1995**, *99* (31), 12021–12024. <https://doi.org/10.1021/j100031a034>.
- (5) Humphrey, W.; Dalke, A.; Schulten, K. VMD - Visual Info Molecular Dynamics. *J. Molec. Graph.* **1996**, *14* (1), 33–38. <https://doi.org/10.1017/CBO9781107415324.004>.